EXPERIMENTAL CELL RESEARCH 326 (2014) 280–294

Available online at www.sciencedirect.com

ScienceDirect

journal homepage: www.elsevier.com/locate/yexcr

Research Article

Traction force microscopy in rapidly moving cells reveals separate roles for ROCK and MLCK in the mechanics of retraction

*Timothy R. Morin Jr., Sean A. Ghassem-Zadeh, Juliet Lee**

Department of Molecular and Cell Biology, University of Connecticut, 91 North Eagleville Road, Storrs, CT 06269, USA

ARTICLE INFORMATION

Article Chronology:
Received 29 January 2014
Received in revised form
15 April 2014
Accepted 18 April 2014
Available online 29 April 2014

Keywords:
Adhesion
Cell motility
Contractility
Mechanics
Retraction
Traction stress

ABSTRACT

Retraction is a major rate-limiting step in cell motility, particularly in slow moving cell types that form large stable adhesions. Myosin II dependent contractile forces are thought to facilitate detachment by physically pulling up the rear edge. However, retraction can occur in the absence of myosin II activity in cell types that form small labile adhesions. To investigate the role of contractile force generation in retraction, we performed traction force microscopy during the movement of fish epithelial keratocytes. By correlating changes in local traction stress at the rear with the area retracted, we identified four distinct modes of retraction. “Recoil” retractions are preceded by a rise in local traction stress, while rear edge is temporarily stuck, followed by a sharp drop in traction stress upon detachment. This retraction type was most common in cells generating high average traction stress. In “pull” type retractions local traction stress and area retracted increase concomitantly. This was the predominant type of retraction in keratocytes and was observed mostly in cells generating low average traction stress. “Continuous” type retractions occur without any detectable change in traction stress, and are seen in cells generating low average traction stress. In contrast, to many other cell types, “release” type retractions occur in keratocytes following a decrease in local traction stress. Our identification of distinct modes of retraction suggests that contractile forces may play different roles in detachment that are related to rear adhesion strength. To determine how the regulation of contractility via MLCK or Rho kinase contributes to the mechanics of detachment, inhibitors were used to block or augment these pathways. Modulation of MLCK activity led to the most rapid change in local traction stress suggesting its importance in regulating attachment strength. Surprisingly, Rho kinase was not required for detachment, but was essential for localizing retraction to the rear. We suggest that in keratocytes MLCK and Rho kinase play distinct, complementary roles in the respective temporal and spatial control of rear detachment that is essential for maintaining rapid motility.

© 2014 Elsevier Inc. All rights reserved.

*Corresponding author.
E-mail address: juliet.lee@uconn.edu (J. Lee).

http://dx.doi.org/10.1016/j.yexcr.2014.04.015
0014-4827/© 2014 Elsevier Inc. All rights reserved.

Introduction

Continuous cell movement consists of repeated cycles of protrusion at the leading edge, with retraction at the rear. This is dependent on the organization of cytoskeletal function such that adhesion formation and protrusive force generation is maximized at the front, while increased contractility and de-adhesion facilitate retraction at the rear [42]. Although the biochemical basis of these processes has been studied for some time, it is still not clear how they are coordinated with one another. An increasing number of studies now show that myosin II dependent contractile force is central to the integration of cytoskeletal function in moving cells [8,49]. An essential part of this process is the coordination of protrusion with retraction, because this will influence both cell speed and mode of movement. Since, protrusion is generally considered to be the first, essential "step" in motility a larger number of studies have focused on this process than on retraction. However, learning more about the regulation of rear detachment is equally important for understanding how cytoskeletal functions are coordinated between the front and rear.

Early studies of motile fibroblasts were the first to demonstrate that retraction can be a major limiting step in cell motility [7,6,14]. The formation of large, stable, focal adhesions at the rear of fibroblasts provides greater resistance to forward movement than weaker more labile ones. Consequently, protrusion and retraction occur as separate phases, resulting in the slow, discontinuous movement that is typical of fibroblasts. In contrast, keratocytes and other fast moving cells types such as leukocytes or *Dicytostelium* amoebae form few or no focal adhesions, which impose less resistance to retraction [28]. This increases the degree of synchrony between protruding and retracting edges, which underlies the rapid, continuous motion of keratocytes. Thus the regulation of rear detachment is a key determinant of cell speed and mode of movement.

A long-standing view is that myosin II dependent contractile forces are directly involved in pulling up the rear edge, and is supported by studies which show that retraction is impaired when myosin II is inhibited [21,54,26]. In addition, myosin II activity has been shown to act in combination with a number of biochemical mechanisms to trigger retraction [9,40,25]. Furthermore, myosin II may indirectly weaken adhesions through force-induced changes in enzyme activity, kinetics [18,51,53] or structural changes in adhesion components [44]. There is evidence to suggest that the mechanism(s) of detachment may vary depending on both substratum adhesiveness and adhesion strength. For example, retraction in fibroblasts is dependent on calpain-induced adhesion disassembly when they are attached to surfaces of high adhesiveness but not when this is low [41]. Similarly, retraction in neutrophils and *Dictyostelium* amoebae is generally dependent on myosin II activity, except when cells are attached to weakly adhesive surfaces [21,15]. Studies of retraction have generally been performed with fibroblastic cells, and so may not accurately reflect the mechanisms used by fast moving cell types.

Changes in intracellular calcium concentration $[Ca^{2+}]_i$ play a key role in regulating retraction, because they can regulate both contractility via MLCK, and adhesion disassembly by activating enzymes such as calpain or calcineurin (Kirfel, 2004). In addition, calcium signals can specify the location and timing of retraction through increasing gradients of $[Ca^{2+}]_i$ toward the cell rear [4] or by transient increases in $[Ca^{2+}]_i$, respectively [33,36,27]. Furthermore, stretch-activated calcium channels (SACs) can trigger calcium transients that induce retraction in keratocytes and *Dictyostelium* amoebae, when the rear becomes temporarily stuck [27,32]. Thus SACs can maintain rapid motility by increasing the degree of synchrony between protruding and retracting edges. It is noteworthy that retraction in leukocytes is also dependent on calcium transients suggesting that they may be particularly important for regulating detachment in cell types whose function depends on rapid movement.

The use of traction force microscopy (TFM) in a variety of cell types has shown that the largest traction forces are located at the rear consistent with their role in retraction [29,35,48,47,20,34]. In ameboid cell types, increased contractility at the rear is thought to facilitate retraction by pulling up the rear or by squeezing the cell forward. In keratocytes, calcium dependent increases in traction stress were shown to facilitate retraction through a combination of increased contractility and adhesion disassembly [11,13]. However, it is still not clear how increased contractility at the rear contributes to retraction, because the relationship between traction stress magnitude and rate of detachment has not been measured directly.

In this study, we have used TFM to measure changes in traction stress at the rear during retraction at high temporal and spatial resolution. In addition, we examined the role of contractility in rear detachment by using inhibitors to modulate calcium dependent and independent regulation of contractility, through MLCK and ROCK, respectively. Comparison of the effects of these treatments on the mechanics of detachment revealed distinct functions for MLCK and ROCK in the respective temporal and spatial regulation of retraction. Our data suggest that modulation of MLCK activity is sufficient to regulate detachment, while Rho kinase localizes retraction to the rear. We propose that this represents a new paradigm for the regulation of detachment, and is of particular importance for fast moving cell types whose function depends on rapid motility.

Methods

Reagents

Stock solutions were made as follows: ML7 (EMD Millipore, MA) at 2 mM in 50% ethanol, Y-27632 (EMD Millipore, MA) at 5 mM in PBS, the active S-enantiomer of blebbistatin at 5 mM in DMSO, calcyculin A at 10 μM in 100% ethanol, and calcimycin (A-23187, free acid, Invitrogen Corporation, CA) at 50 mM in DMSO. Before use, all inhibitors were made up at twice their final working concentration so that this was halved when an equal volume was added to the cell chamber. Inhibitor solutions were made up in RPMI 1640 (Sigma-Aldrich Corporation, MO) supplemented with ~2% serum, and syringe-filtered before use.

Preparation of polyacrylamide substrata

Polyacrylamide (PA) gels were prepared as described in detail elsewhere [43] with some minor modifications. Briefly, 22 mm^2 square, zero thickness coverslips (Electron Microscopy Sciences, Hatfield, PA) were "activated" in order to facilitate binding of the polyacrylamide gel to the coverslip. Solutions of 40% polyacrylamide and 2% bis-acrylamide (Bio-Rad, Hercules, CA) were made into a

working stock solution containing of 16.67% acrylamide and 0.167% bis-acrylamide, then degassed for 20 min under house vacuum. A polymerization mixture (500 ul) was made consisting of; 150 μl of the working polyacrylamide/bis-acrylamide stock solution, 2.5 μl ammonium persulfate (10%), 0.75 μl TEMED, 5 μl red (excitation/emission 580/605 nm) fluorescent microspheres (diameter=0.2 nm, Invitrogen Corp.) and 341.75 μl ddH_2O. A 10 μl drop of the polymerization mixture was placed on a microscope slide and gently overlaid with an activated coverslip. After 20 min, the coverslip was peeled up from the microscope slide and stored face-down in a 100 μl drop of ddH_2O within a sealed Petri-dish, at 4 °C, until further use. Polyacrylamide gels made in this fashion were ~20 μm in thickness with an elastic shear modulus G' of 600 Pa. A surface coating of fibronectin (1 mg/ml, Sigma-Aldrich Corp.) was covalently linked to the polyacrylamide gel using the heterobifunctional cross-linker sulpho-SANPAH (Pierce, Rockford, IL).

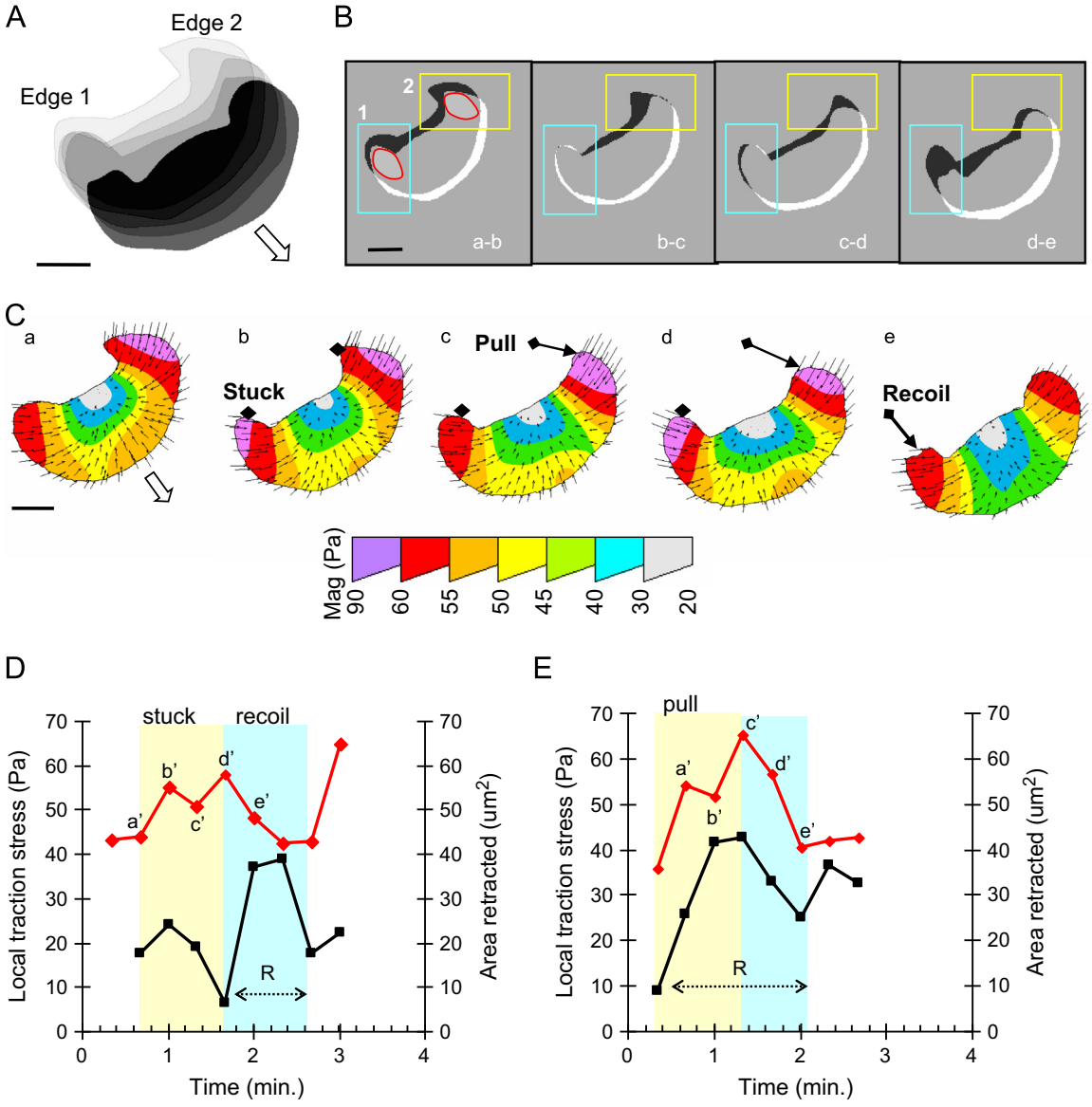

Fig. 1 – TFM reveals distinct modes of retraction in moving keratocytes. (A) Overlay of cell outlines at 20 s intervals during a recoil (edge 1) and a pull type retraction (edge 2) in a moving keratocyte. (B) A series of difference images of the cell in A, at 20 s intervals, showing areas retracted (black) and protruded (white). Boxed regions 1 and 2, show where measurements of area retracted (Ar) and local traction stress (TS*l*, red ovals) where taken from. (C) Color coded traction vector maps (a–e) of the cell in A, showing changes in magnitude of traction stress associated with recoil and pull type retractions. Black diamonds mark the position of the rear edge at the onset of retraction, and arrows indicate the path of retraction. (D) Plots of TS*l* (red line) and Ar (black line) from edge 1 in panel A, during the recoil retraction shown in B and C. Data points (a'–e') correspond to measurements taken from the traction maps (a–e) in C. Colored regions represent periods when the rear edge is stuck (yellow) and during retraction (blue). (E) Plots of TS*l* and Ar from edge 2 during the pull type retraction shown in B and C. Colored regions represent periods when TS*l* and Ar are increasing or pulling (yellow) and decreasing (blue). The duration of retraction (R) is indicated by a double-headed arrow. Direction of movement is indicated by an open arrow. Bars, 10 μm.

Traction force microscopy

Fish epithelial keratocytes were cultured from Molly fish *Poecillia sphenops* scales as described previously [27]. After ~2–3 days in culture cells were re-plated onto polyacrylamide gels, and mounted in a cell culture chamber with 400 μl RPMI medium supplemented with (~2%) serum without antibiotics or anti-fungal agents, to reduce background fluorescence. Dual DIC and fluorescence imaging of red marker beads was performed using an Andor Revolution spinning disc confocal system, consisting of a Nikon Eclipse Ti microscope with a Plan APO 60×, 1.4 N.A. oil immersion objective. Fluorescence excitation was achieved using a 561 nm laser, and emitted fluorescence was collected using a red fluorescence emission filter (607/36 nm). Images were acquired using an iXon897 EMCCD camera (Andor Technology, plc) driven by Andor iQ imaging software for image acquisition and hardware control. Paired DIC and fluorescence images of the cell and marker beads, respectively, were collected between 5 and 20 s, for several minutes, from 1 to 4 fields of view using a MS-2000 motorized stage (Applied Scientific Instrumentation, Eugene, OR). For inhibitor treatments, cells were first imaged for ~3 min, before adding an equal volume (~400 ul) of the inhibitor solution, at double the final concentration, to the cell culture chamber.

Data analysis

The average cell speed was calculated by tracking the middle of the back cell edge using ImageJ software (W.S. Rasband, NIH), and then dividing the total distance moved by time. For each inhibitor treatment, 8–10 keratocytes were tracked for a period of ~5 min before, and ~15 min after treatment. The persistence of cell movement was calculated by dividing the net distance by the total distance moved.

Calculation of the traction stresses generated by moving keratocytes, and plots of traction vector maps were made using the LIBTRC traction analysis software written and developed by Professor Micah Dembo at Boston University [10]. Measurements of local traction stress were taken from 8 bit monochrome images generated by converting traction stress magnitude at each pixel to a grey value. Local traction stress (TS*l*) at the retracting cell margins was obtained by averaging the grey values within a small oval region at each retracting edge, for every image in the sequence (Fig. 1B).

The area retracted (Ar) for each time point was obtained from within a rectangular region positioned over the lateral rear cell edges of difference images generated from successive cell outlines (Fig. 1B). The "Region Measurement" tool in MetaMorph (Molecular Devices, LLC, CA) was then used to measure the area of black regions that represent the area retracted (Ar) during 10–20 s intervals. To verify periods of increased retraction rate, graphs of Ar over time were compared with those obtained from manual tracking of the retracting edges in the original DIC images, using the "Track Points" tool in MetaMorph. Periods of increased retraction rate were defined by the values of Ar at time points corresponding to the onset of detachment (pre), peak and post retraction. These same time points were used to find the corresponding values of TS*l* during retraction. The baseline values for Ar and TS*l* were obtained ~20 s prior to the pre retraction value. Different modes of retraction were identified by comparing the changes in TS*l* (ΔTS*l*) with the change in area retracted (ΔAr) between pre to peak values of these parameters (Fig. 2).

The efficiency of each retraction type, E was calculated by obtaining the group average of the ratio, ΔAr to ΔTS*l*, for every retraction. Negative values of E were considered to be more efficient than positive ones, because the increase in retraction rate is accompanied by a decrease in TS*l*. The effects of each inhibitor treatment was quantified by first calculating the average retraction efficiency E_{avg}, without identifying specific periods of increased retraction rate, or considering retraction type. Since changes in retraction rate are associated with fluctuations in TS*l*, we used the Standard Deviation (s.d.) of all values of Ar and TS*l*, for pre and post treatment periods. Thus E_{avg}=(s.d. Ar)/(s.d.TS*l*) and the fold-change in average retraction efficiency (ΔE_{avg}) resulting from drug treatment is given by, $\Delta E_{avg}=(E_{avg}$ post)/(E_{avg} pre). The average change in adhesion threshold, ΔAT_{avg}, is given by ΔAT_{avg}=TS*l* post–TS*l* pre, where TSl_{avg} is the mean of all values of TS*l* before (pre) or after (post) treatment.

Results

Moving keratocytes exhibit distinct mechanical modes of retraction

To examine the role contractile force generation in retraction, TFM was performed with untreated keratocytes crawling on highly flexible polyacrylamide gels (Movies 1 and 2). These data were used to generate traction maps at high temporal and spatial resolution, from which we obtained measurements of the changes in local traction stress (TS*l*) that occur at the rear during retraction (Fig. 1, Movie 3). To ascertain how contractile force mediates detachment, we compared changes in TS*l* with area retracted (Ar). In addition, we recorded the magnitude of TS*l* at which each period of retraction is initiated that we refer to here as the "adhesion threshold". As described previously, the adhesion threshold can provide a measure of rear attachment strength, because it represents the maximum contractile force that adhesions can withstand before detachment [11]. Using this approach, we identified four mechanical modes of detachment in untreated

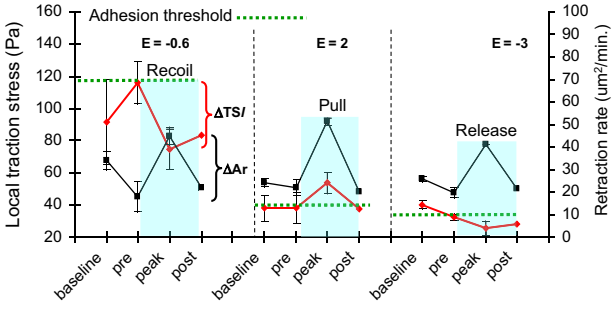

Fig. 2 – A characteristic sequence of changes in TS*l* and Ar is associated with each retraction type. Plots of the average TS*l* and associated Ar for recoil (n=6), pull (n=15) and release (n=9) type retractions occurring in 9 untreated keratocytes, during 3–4 min of movement. The change in magnitude of TS*l* (ΔTS*l*, red bracket) that accompanies the change in rate of Ar (ΔAr, black bracket) is indicated. The average adhesion threshold (dotted green line) and period of retraction (blue region) are shown. *E* is the retraction efficiency for a given retraction type. Error bars, S.E.

cells that we term recoil, pull, release and continuous (Figs. 1 and 2). Each retraction type is characterized by a distinct sequence of changes in magnitude of TS*I* with respect to retraction rate, as follows:

Supplementary material related to this article can be found online at http://dx.doi.org/10.1016/j.yexcr.2014.04.015.

A recoil retraction is preceded by a period of increasing TS*I* and decreasing Ar as the rear cell margin becomes transiently "stuck" (Fig. 1B, C and D, Movie 3). When TS*I* exceeds the adhesion threshold the rear edge detaches abruptly, together with a sharp increase in Ar and a decrease in TS*I*. On average, recoil retractions have the highest adhesion threshold (~116 Pa) and occur after a ~40 Pa rise in average TS*I*. This is equivalent to a 20% increase above baseline TS*I*, which is higher than for other retraction types, as might be expected for the detachment of stronger adhesions (Fig. 2). Pull type retractions occur at a significantly lower adhesion threshold (~45 Pa), which is equal to the baseline value of TS*I*, consistent with the detachment of weaker adhesions. This retraction type is characterized by a simultaneous rise in TS*I* and Ar toward a maximum, followed by a decrease in both values as the period of retraction ends (Fig. 1B, C and E, Movie 3). Unlike recoil retractions, release-type retractions are preceded by a decrease in TS*I*, which triggers detachment when this reaches a critical minimum adhesion threshold (Fig. 2). As retraction proceeds, TS*I* continues to decrease, while Ar increases from the onset of detachment, until the peak retraction rate is reached. The average adhesion threshold of release type retractions is ~37 Pa, and since this is lower than baseline TS*I* suggests that this mode of detachment results from a period of adhesion weakening. Continuous type retractions differ from all the others, because they can occur without any detectable change in TS*I* (data not shown). Despite these differences in the mechanics of detachment, the average area retracted for each retraction type was the same (~30–40 um^2) except for the smaller (~26 um^2) release type retractions. In addition, the average duration of all retraction types was (~30 s) which is expected since keratocytes are usually highly motile.

The association of recoil retractions with a high adhesion threshold suggests that more contractile force might be required per unit area retracted than retraction types with lower adhesion thresholds. To determine the effectiveness of contractile force in triggering detachment, the change in TS*I* (ΔTS*I*) and accompanying increase in Ar (ΔAr) was measured and used to calculate retraction efficiency, *E*, for every retraction within each group of retraction type in untreated cells (Fig. 2). Release type retractions ($E=-3$) were the most efficient, because they were associated with a small negative ΔTS*I*. Pull type retractions were the least efficient ($E=2$) because they are accompanied by a positive ΔTS*I* and recoil retractions were of intermediate efficiency ($E=-0.6$). Together, these findings show that the mode of retraction is related both to the baseline level of TS*I*, and to the mechanosensory response of rear adhesions to changes in contractile force. This suggests that the role of contractile force may vary depending on the strength of rear attachments.

Inhibition of MLCK induces release type retractions by lowering the adhesion threshold

The calcium dependent regulation of contractility via MLCK is required for retraction in neutrophils, since its inhibition with ML7 prevents retraction [15]. However, ML7 treatment of keratocytes induces retraction suggesting that this is due to adhesion weakening at the rear [22]. Another possibility is that ML7 does not inhibit MLCK sufficiently to prevent retraction in keratocytes, or that it does not play a major role in regulating detachment. We addressed this question by treating keratocytes with 5 μM ML7, and used high resolution TFM to detect any change in the mechanics of retraction (Fig. 3, Movie 4). Within ~40 s, a rapid drop in traction stress occurred throughout the cell, together with decreased values of TS*I* at the rear edges, followed by a release type retraction ~40 s after that. All retractions initially induced by ML7 were of the release type (Fig. 8A) and involved an average decrease in TS*I* of ~50 Pa, which is equivalent to a 55% reduction in the adhesion threshold compared with the pretreatment value (Fig. 8B). This large decrease in traction stress led to a temporary halt to cell movement, due to the loss of traction stress asymmetry [31] between the front and rear of the cell. However, after ~4.5 min cells repolarized and continued movement at pretreatment speeds (Fig. 8C) but with decreased persistence (Fig. 8D). Nevertheless, the average retraction efficiency increased by 7-fold. These findings suggest retraction is due to adhesion weakening that is associated with the significant decrease in TS*I* at the rear, and illustrates the importance of MLCK dependent contractility in regulating attachment strength.

Supplementary material related to this article can be found online at http://dx.doi.org/10.1016/j.yexcr.2014.04.015.

Rho kinase activity is not required for detachment but is necessary for limiting retraction to the rear

Rho kinase activity has been shown to be pivotal for retraction, and the maintenance of polarity in many cell types [38,26,1]. In addition, traction force generation in fibroblasts is dependent on Rho kinase [3]. Since keratocytes exhibit a highly polarized, directed mode of movement, we sought to determine the role of Rho kinase dependent contractility in retraction. We performed TFM in keratocytes treated with 5 μM of the Rho kinase inhibitor, Y27632 (Fig. 4, Movie 5) and found that in contrast to fibroblasts, this did not inhibit retraction (Fig. 4A and B). On the contrary, retraction continued at the lateral cell margins, as shown in this example, a recoil retraction occurs on the left side and two pull type retractions are seen on the right (Movie 5). Consistent with its failure to inhibit retraction, Y27632 treatment did not lead to any change in the proportion of retraction types (Fig. 8A) or to the average change in adhesion threshold and retraction efficiency (Fig. 8B). Instead, the most striking effect was the rapid loss of cell polarity that began ~25 s after treatment. As shown here, a small protrusion developed at the rear, which continued to enlarge until the cell lost polarity (Fig. 4C, panel b–d). Cells remained apolar for ~6 min after treatment, before becoming motile again. However, Y27632 treated cells made frequent changes in direction, which led to a significant reduction in persistence and consequently, cell speed (Fig. 8C and D). Together, these data suggest that Rho kinase activity is not essential for retraction but is required for maintaining cell polarity, which in turn, is necessary for the rapid, highly directed movement exhibited by keratocytes.

Supplementary material related to this article can be found online at http://dx.doi.org/10.1016/j.yexcr.2014.04.015.

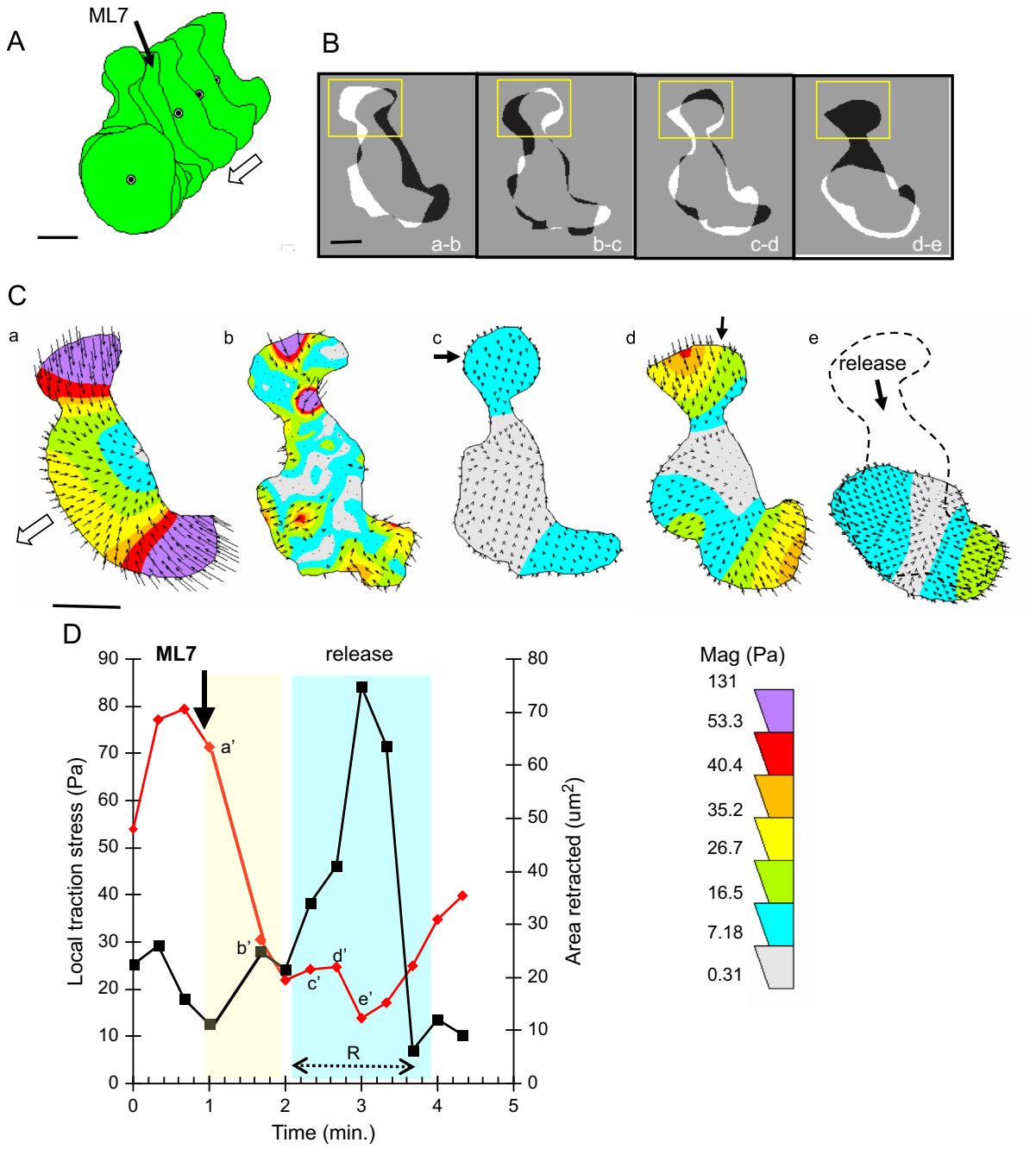

Fig. 3 – Inhibition of MLCK induces retraction by lowering the adhesion threshold. (A) Stacked cell outlines at 20 s intervals from a keratocyte moving in the direction indicated (open arrow) before and after the addition of ML7. (B) A series of difference images obtained from the cell in A, shortly after treatment, in which a release type retraction occurs at the right rear margin (boxed region). Black and white regions represent areas retracted and protruded, respectively. (C) A series of traction vector maps (a–e) corresponding to the outlines in B. A drop in TS*l* occurs is shown in map b that initiates a release retraction maps c and d (arrows) followed by detachment, map e. The total area retracted is represented by the dashed cell outline of the cell in map b, overlaid on map e. (D) Plots of TS*l* (red line) and Ar (black line) within the boxed region, shown in B. Data points (a'–e') correspond to measurements obtained from the traction maps in (a–e) in C. The decrease in TS*l* (yellow region) is followed by an increase in the rate of retraction (blue region). The duration of retraction (R) is indicated by a double-headed arrow. Bars, 10 μm.

Myosin II activity is not required for retraction when the adhesion threshold is very low

Inhibition of either MLCK or Rho kinase may not completely abolish contractility, because these enzymes act upstream of myosin II. Our observation that keratocytes can still retract following ML7 or Y27632 treatment could be due to residual contractility. Therefore, we used blebbistatin, a potent, specific inhibitor of myosin II ATPase [30] to determine whether this could inhibit retraction in keratocytes. Treatment with 50 μM blebbistatin led to an immediate, yet

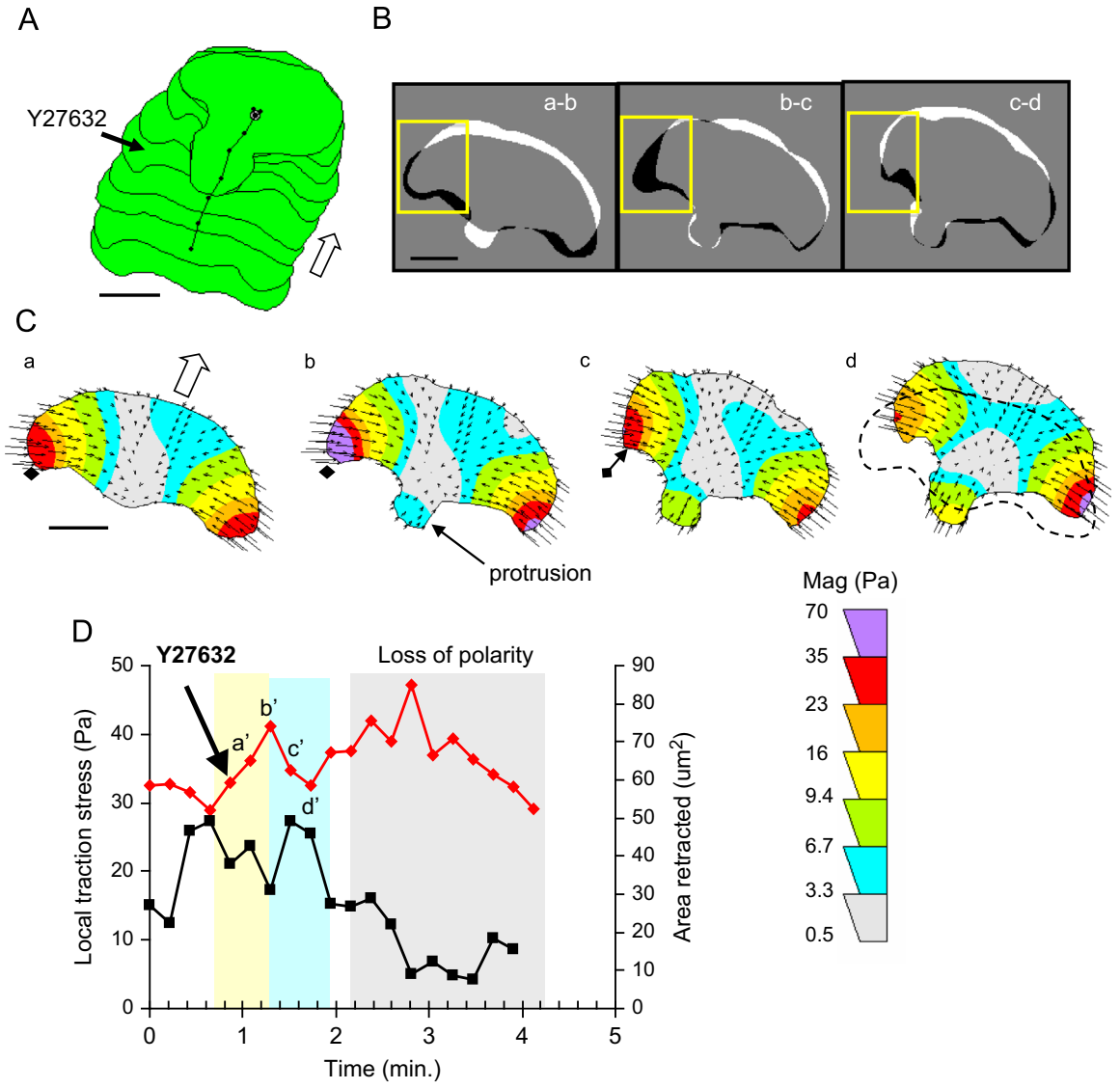

Fig. 4 – Inhibition of Rho kinase leads to a loss of cell polarity. (A) Stacked cell outlines at 26 s intervals from a keratocyte moving in the direction indicated (open arrow) before and after the addition of Y27632. (B) A series of difference images obtained from the cell outlines in A, immediately after treatment with Y27632. Black and white regions represent areas retracted and protruded, respectively. (C) A series of traction vector maps (a–d) corresponding to the outlines in B. A protrusion develops at the rear, map b, and a recoil retraction occurs on the left edge, map c. Black diamonds represent the position of the rear edge at the onset of retraction, and the arrow indicates the path of retraction. The total area retracted is represented by the dashed cell outline of the cell in map a, overlaid on map d. (D) Plots of TS*l* (red line) and Ar (black line) obtained from the left lateral edge (boxed region in B) before and after the addition of Y27632. Data points (a'–d') correspond to measurements taken from the retracting edge in traction maps (a–d) in C. The left edge becomes temporarily stuck (yellow region) prior to a recoil retraction (blue region) and is followed by a loss in polarity (grey region). Bars, 10 um.

Fig. 5 – Retraction can occur without myosin II activity when the adhesion threshold is very low. (A) Stacked cell outlines at 10 s intervals from a keratocyte moving in the direction indicated (open arrow), before and after the addition of blebbistatin. (B) Stacked cell outlines at 5 s intervals, from the cell in A, ~12 min after blebbistatin treatment. (C) A series of traction vector maps corresponding to the outlines of the cell in A, shortly before and after blebbistatin treatment. The total area retracted is represented by the dashed cell outline of the cell in map a, superimposed on map c. Release type retractions occur at the rear edges (arrows). (D) A series of traction vector maps corresponding to the outlines of the cell shown in B. Black diamonds represent the position of the rear edge at the onset of retraction, and the arrow indicates the path of retraction. The total area retracted is shown by the dashed cell outline of the cell in map d, superimposed on map g. (E) Plots of TS*l* (red line) and Ar (black line) obtained before, and after treatment (boxed regions in panels C and D). Pretreatment plots show part of a pull type retraction (yellow region) followed by release and continuous retractions, post treatment (blue regions). Data points (a'–c') and (d'–g') correspond to the traction maps in C and D, respectively. Bars, 10 μm.

temporary halt to cell movement without any change in cell shape, for ~30–60 s (Fig. 5A, Movie 6). During this time, TS*I* at the rear edges decreased by ~43% and was accompanied by release type retractions (Fig. 5C and E, data points a'–c'). In a similar manner to ML7 treatment, the normal asymmetric distribution of traction stresses was lost, which contributed to a decrease in persistence of movement (Fig. 8D). Over the next several minutes, cell polarity was re-established and new protrusions started to form as cells regained motility (movie 6 Movie 6). At this time, TS*I* had decreased to very low (~10 Pa) levels, corresponding to 90% drop in the average

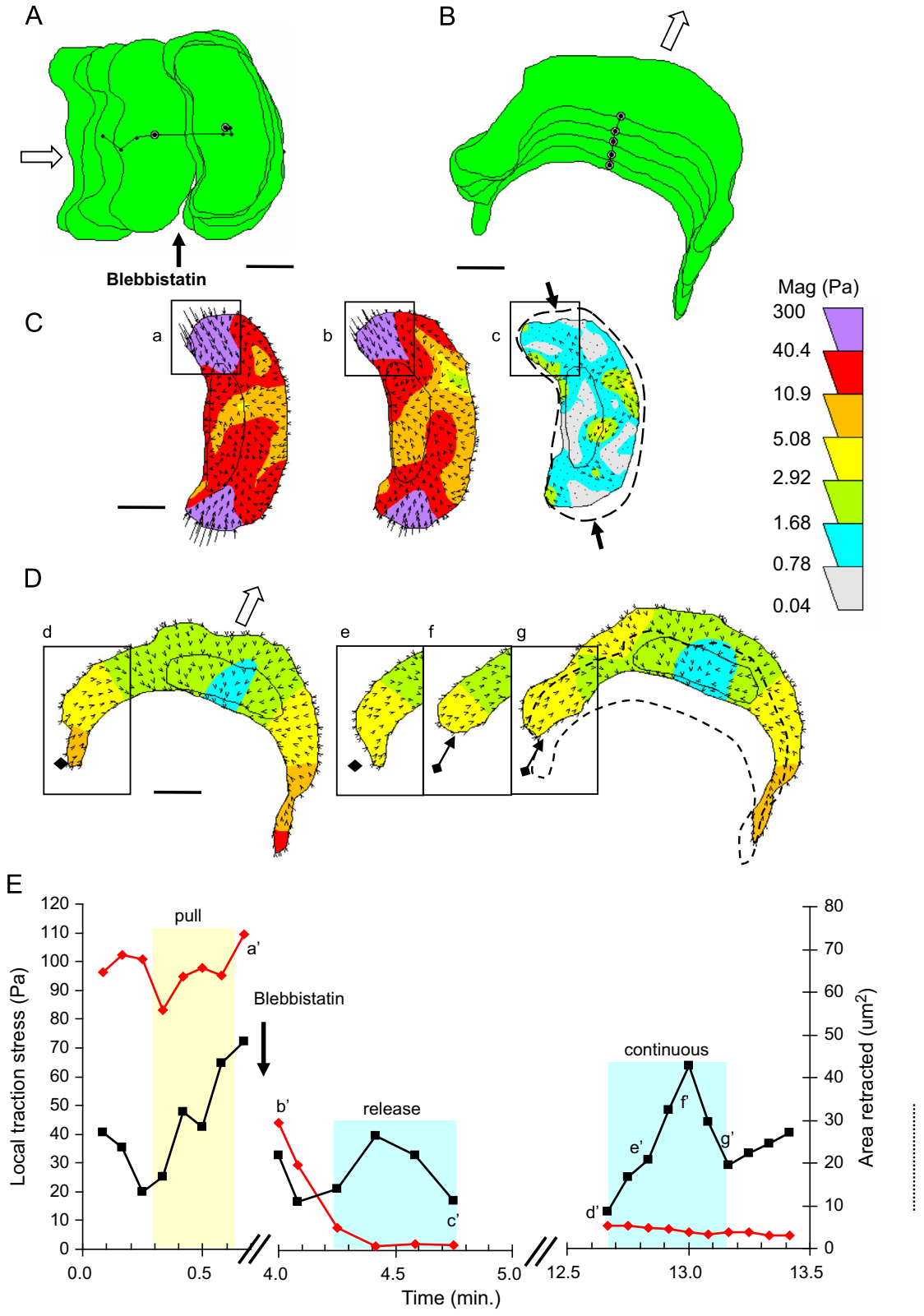

adhesion threshold compared with pre-treatment values (Fig. 8B). By 12 min after treatment, a dramatic increase in cell extensibility was evident that promoted the development of extremely elongated cells, often with multiple lamellae (Fig. 5B and D). At this time, all retractions were of the continuous type (Fig. 8A) and occurred without any detectable change in TS*I* (Fig. 5E, data points d'–g'). In addition, the average retraction efficiency increased ~6 fold compared to the pretreatment value (Fig. 8B). Despite their unusual morphology, blebbistatin treated keratocytes were still capable of movement at a similar rate to untreated cells (Fig. 8C). Together these data show that myosin II dependent contractility is not required for retraction, when adhesions are very weak.

Supplementary material related to this article can be found online at http://dx.doi.org/10.1016/j.yexcr.2014.04.015.

Calyculin A reduces the efficiency of retraction by raising the adhesion threshold

Although retraction in keratocytes can occur in response to a reduction in contractility, the question remains of how myosin II dependent contractile forces promote detachment. To approach this question, we used 2.5 nM calyculin A to increase contractility in a calcium independent manner. Within ~1 min after treatment, retraction occurred along most of the cell margin, so that cells became compact and irregular in shape (Movie 7). This loss of cell polarity led to a temporary halt to cell movement and was associated with an increase in traction stress throughout the cell. Increased traction stress at the cell front, often caused the lamella to collapse, together with a loss of the normal asymmetric pattern of traction stress (Fig. 6A and B). By ~6 min after treatment, cell motility resumed but speed and persistence were reduced (Fig. 8C and D). At this time, 90th percentile traction stress had increased by 200%, and pull type retractions were the predominant mode of detachment (Fig. 8A). As shown in this example, retractions occurred over large sections of the lateral cell edges (Fig. 6C and D, Movie 7). Each retraction was accompanied by a ~47 Pa increase in TS*I*, equivalent to a 78% increase above post treatment baseline values. These retractions were superimposed upon a progressive increase in the baseline TS*I* that reached a total of 400% above pretreatment baseline values, after ~5 min (Fig. 6E). It is noteworthy that despite this increase in contractility, the average retraction rate remained lower than in untreated cells, such that the retraction efficiency for this example is reduced four-fold. On average, calyculin A treatment led to an increase in the adhesion threshold of ~40 Pa that represents a 200% increase compared with untreated cells, and was accompanied by a 50% reduction in the average retraction efficiency (Fig. 8B). These data show that a calcium independent increase in contractility can induce retraction but is inefficient, because this leads to a progressive increase in adhesion threshold, so that more force is required per unit area of detachment.

Supplementary material related to this article can be found online at http://dx.doi.org/10.1016/j.yexcr.2014.04.015.

Calcimycin maintains retraction efficiency by limiting increases in the adhesion threshold

We have previously shown that calcimycin can mimic a stretch-induced calcium transient by triggering a retraction that is preceded by an increase in 90th percentile traction stress [11,13]. However, we could not determine whether increased contractility had a direct or indirect role in detachment. To approach this question, we treated keratocytes with 5 μM calcimycin, and observed how this affected the mechanics of detachment. Consistent with our previous findings, calcimycin led to a rapid increase in traction stress followed ~40 s later by a retraction (Fig. 7). In this example, two consecutive recoil retractions occur at the left lateral edge, the first of which is initiated within 10 s after treatment. Each retraction was preceded by a large, rapid increase in TS*I* together with a reduced retraction rate, followed by an abrupt detachment and a decrease in TS*I* (Fig. 7D). In contrast to calyculin A, calcimycin induced increases in TS*I* and subsequent areas of detachment were localized to the rear, so that cell speed and polarity were maintained (Figs. 7A–C, 8C and D). In general, the proportion of retraction types resembled that of untreated cells (Fig. 8A) and unlike calyculin A treatment, occurred without a net increase in adhesion threshold, or any change in average retraction efficiency, compared with untreated cells (Fig. 8B). These data indicate that calcium dependent increases in contractility facilitate detachment without raising the adhesion threshold, and thus maintain retraction efficiency.

Discussion

We have identified distinct mechanical modes of detachment by correlating changes in local traction stress with the kinematics of retraction. Each retraction type provides insight into how contractile forces are mediating detachment. For example, the "stick-release" kinematics of recoil retractions, together with the fact that they occur following an increase in TS*I* suggests that increased contractility reinforces adhesions prior to detachment. In contrast, release type retractions are preceded by a decrease in TS*I* prior to detachment, indicative of adhesion weakening. The concomitant increase in TS*I* during pull type retractions suggests that the increase in contractility is directly involved in detachment. Inhibitor studies revealed that MLCK activity was primarily involved in regulating rear detachment, over short time scales. Surprisingly, Rho kinase was not required for detachment, as has been reported for many other cell types, but was essential for localizing retraction to the rear. We propose that the distinct, complementary roles of MLCK and Rho kinase provide respective temporal and spatial control of rear detachment that is essential for maintaining rapid motility (Fig. 9).

The resemblance of recoil retractions in keratocytes to those observed in fibroblasts [7,6] suggests that detachment occurs when contractile force is sufficient to rupture adhesions. However, our observation that a rise in TS*I* precedes detachment is consistent with a period of adhesion reinforcement, especially since we also observe a decrease in retraction rate as the rear becomes stuck. Although counterintuitive, adhesion reinforcement may be necessary to trigger some auxiliary mechanism that promotes detachment. Since stretch-induced calcium transients often precede recoil retractions [11,13], it is possible that they could activate calpain, which would disassemble adhesions enzymatically, thus inducing detachment. However, inhibition of calpain had no effect on retraction in keratocytes attached to gelatin gels [12]. Although the activation of calpain remains a possibility, we believe this not important for detachment in keratocytes,

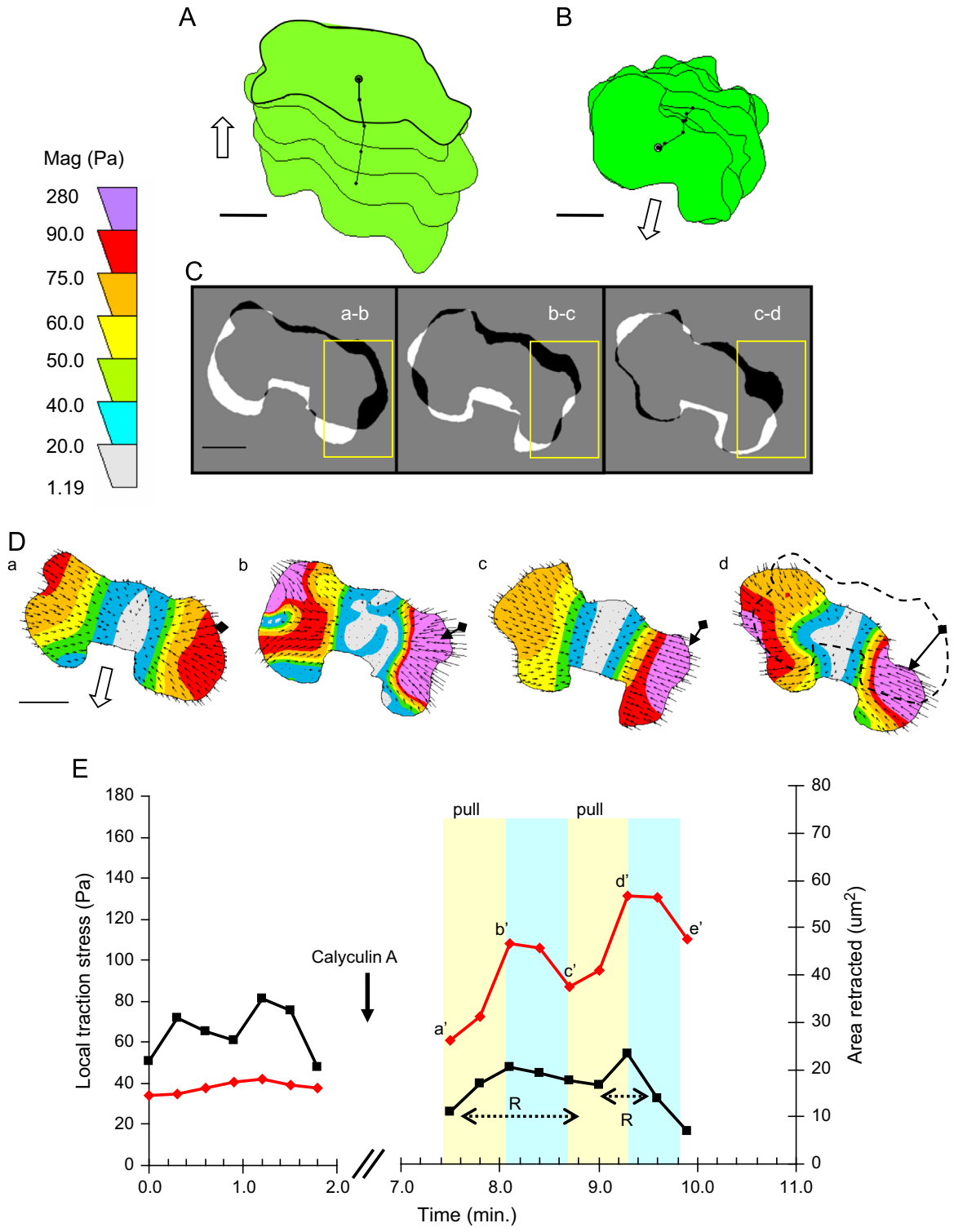

Fig. 6 – Calyculin A promotes inefficient pull type retractions. (A) Stacked cell outlines at 18 s intervals of an untreated keratocyte moving in the direction indicated (open arrow). (B) Stacked cell outlines at 18 s intervals of the cell in A, ~6 min after treatment with 2.5 nM calyculin A. (C) A series of difference images obtained from the cell outlines in B, during two pull type retractions on the left side (boxed region). Black and white regions represent areas retracted and protruded, respectively. (D) A series of traction vector maps corresponding to the image sequence of the cell in C. Black diamonds represent the position of the rear edge at the onset of retraction, and the arrow indicates the path of retraction. The total area retracted is shown by the dashed cell outline of the cell in map a, overlaid on map d. (E) Plots of TS*I* (red) and Ar (black) corresponding to the image sequence in A before, and B after treatment. Data points (a'–d') correspond to the traction maps (a–d) in D. For each pull type retraction (R, double-headed, dotted arrows) a period of increasing TS*I* and Ar (a'–b') and (c'–d', yellow regions) and respective periods of decreasing TS*I* and Ar (b'–c') and (d'–e', blue regions) are shown. Bars, 10 μm.

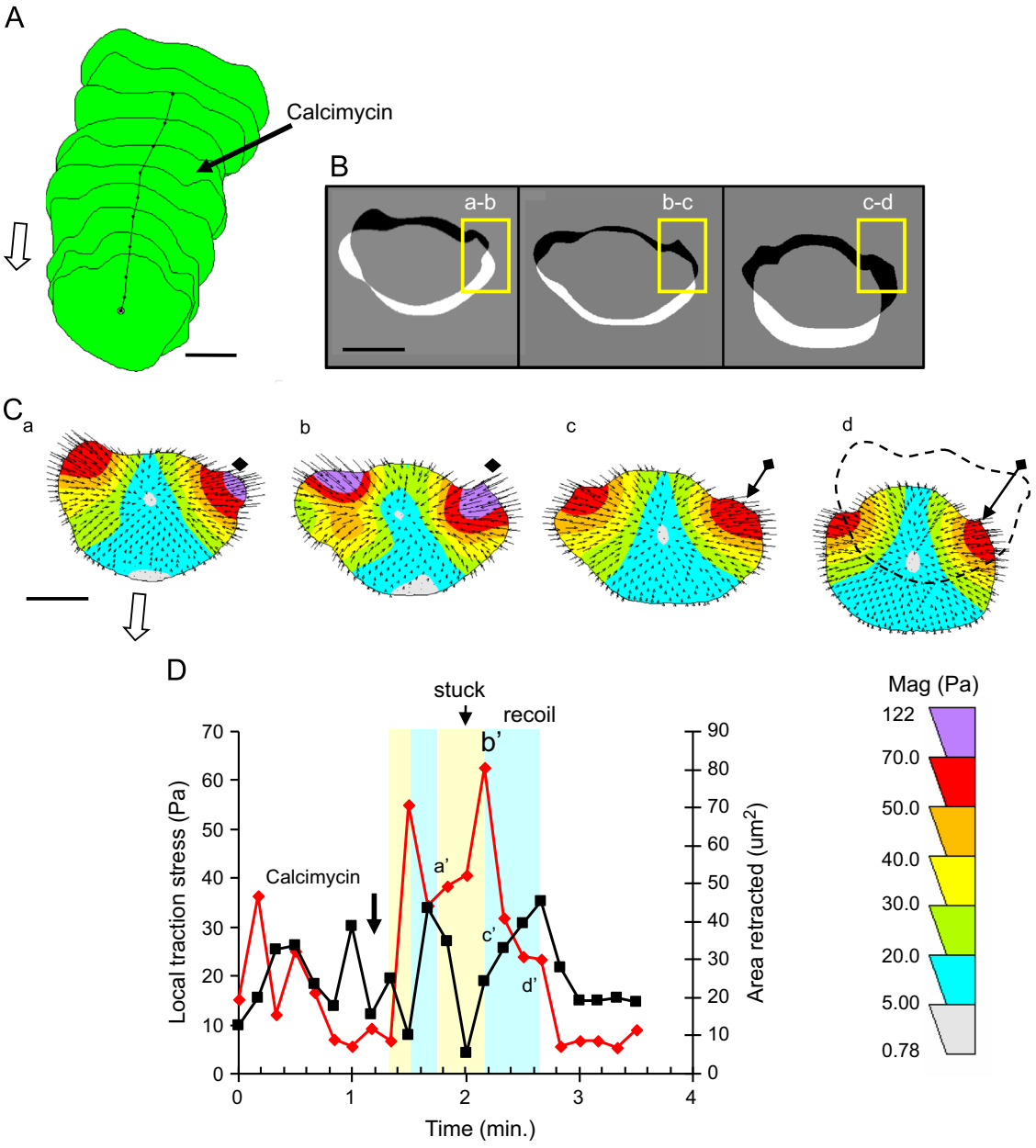

Fig. 7 – Calcimycin induces retraction without any net change in adhesion threshold. (A) Stacked cell outlines, at 10 s intervals from a cell moving in the direction indicated (open arrow) before and after the addition of calcimycin. (B) A series of difference images corresponding to the cell outlines shown in A, ~40 s after the addition of calcimycin. Black and white regions represent areas retracted and protruded, respectively. (C) A series of traction vector maps corresponding to the sequence shown in B showing a recoil retraction on the right side (boxed region in B). Black diamonds represent the position of the rear edge at the onset of retraction, and the arrow indicates the path of retraction. The total area retracted is shown by the dashed cell outline of the cell in map a, overlaid on map d. (D) Plots of TS*l* (red) and Ar (black) before and after treatment, corresponding to the sequence shown in A. Data points (a'–d') were obtained from the traction maps (a–d) in C. This shows the second of two recoil retractions, on the left side. Each retraction consists of period when the edge is stuck (yellow) followed by a retraction (blue). Bars, 10 μm.

because their adhesions are relatively weak, and are weakened further when attached to flexible surfaces. In support of this possibility, calpain is not required for retraction in fibroblasts when they are attached to weakly adhesive surfaces [41]. Therefore, calpain activity may only be required when the proteolysis of large focal adhesions is necessary for rear detachment.

Another mechanism by which adhesion reinforcement might promote detachment is through force-dependent adhesion disassembly. Examples of such mechanisms include: lengthening the residency time of FAK at adhesion sites [18], shortening the cycle of adhesion formation and disassembly [45], increasing the retrograde flow of actin [17] and increasing the dissociation rate of adhesion components [53]. The advantage of force-induced adhesion disassembly at the rear is that it can trigger detachment locally where adhesions are under the most stress and before they begin to limit forward movement. Thus force induced adhesion

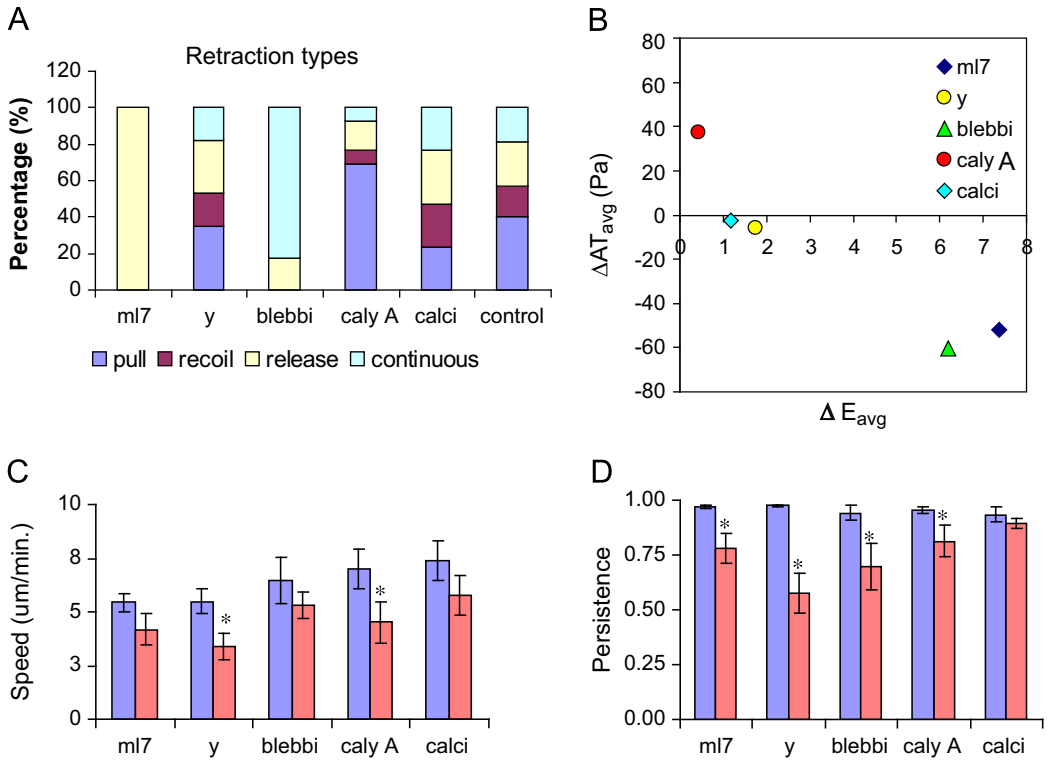

Fig. 8 – Comparison of the effects of inhibitor treatments on the mechanics of retraction and cell motility. (A) Stacked histogram showing the proportion of retraction types observed following each inhibitor treatment, compared with untreated (control) cells. (B) Graph of the change in average adhesion threshold (ΔAT_{avg}) against the change in average retraction efficiency (ΔE_{avg}) resulting from inhibitor treatment. Data were collected from ~20 min observations of 3–4 keratocytes for each treatment, where the number of retractions analyzed is: $n=9$ for ml7, $n=17$ for Y27632 (Y), $n=23$ for blebbistatin (blebbi), $n=13$ for calyculin A (caly A), $n=17$ for calcimycin (calci), and $n=38$ for untreated control cells. (C) Histogram showing the effect of inhibitor treatment on cell speed. Data were obtained from tracking the position of 8–10 cells, over a period of ~15 min, for each condition. (D) Histogram showing the effect of inhibitor treatment on persistence of cell movement. Asterisks indicate statistically significant differences compared with untreated cells ($P<0.05$), using Student's *t*-test, assuming equal variances. Error bars, S.E.

disassembly could provide negative feedback on reinforcement to limit rear attachment strength and promote detachment. Comparison of calcimycin induced retractions with the effects of calyculin A suggest that calcium dependent increases in contractility are important for regulating rear detachment through force induced adhesion disassembly.

The predominant mode of detachment in untreated keratocytes is the pull type retraction, and since these occur at a low adhesion threshold, they most likely represent the detachment of weakly, reinforced adhesions. However, our finding that pull type retractions can occur at a high adhesion threshold, as seen following calyculin A treatment suggests that the role of contractile force varies depending on rear attachment strength. For example, at a low adhesion threshold, small increases in TS*l* may be sufficient for detachment, without triggering adhesion reinforcement, as long as they can overcome viscous drag between the ventral cell surface and the substratum. At a higher adhesion threshold, contractile forces might contribute to inward adhesion sliding by simultaneously triggering reinforcement and disassembly at respective inner and outer edges of individual attachments [46]. This possibility is supported by the observation of inward sliding of adhesion complexes at the retracting edges of keratocytes [2] and similarly shaped fibrosarcoma cells [39]. At the highest adhesion threshold, when adhesions are already reinforced, contractile forces could trigger detachment if they are sufficient to rupture adhesions. This is exemplified by the effects of calyculin A in which increasing contractile forces are sufficient to pull up the rear but are inefficient due to the progressive increase in TS*l*.

One of the striking differences between retraction in keratocytes and fibroblastic cells is that it can occur following a decrease in TS*l*. This contradicts the long-standing view that myosin II activity is required for retraction but is consistent with the finding that retraction in keratocytes can occur when contractility is reduced below an essential minimum [22]. As such, it is possible that release type retractions represent a novel mode of detachment specific to fast moving cell types. Another major difference between keratocytes and fibroblasts is their response to blebbistatin. As seen in this study and observed by others, keratocytes can retract and remain motile following blebbistatin treatment [16,52], whereas these processes are inhibited in fibroblasts [19]. These findings provide support for the idea that myosin II activity is not required for retraction if cell attachments are very weak. Under these circumstances, it is possible that protrusive forces generate enough membrane tension to withdraw the rear edge [24,16]. However, the movement of blebbistatin treated keratocytes is clearly abnormal as cells become increasingly elongated, and develop multiple protrusive regions. Therefore, although

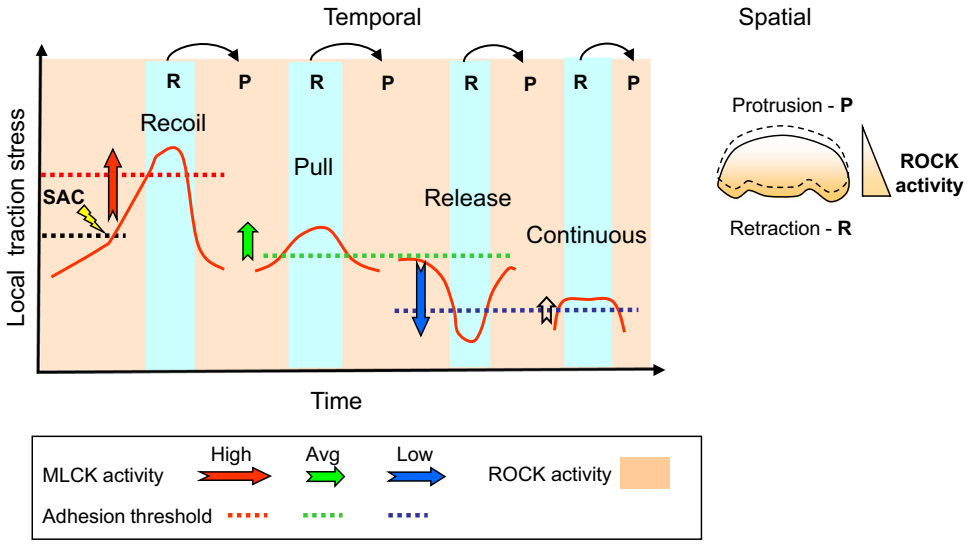

Fig. 9 – Diagram illustrating how the separate roles of MLCK and Rho kinase could provide respective, temporal and spatial regulation of detachment. Fluctuations in MLCK activity over time (colored block arrows) regulate TS*I* (red line) at the rear, inducing different retraction types (blue regions) depending on the adhesion threshold (colored, dotted lines). At the highest adhesion threshold, SACs trigger calcium transients in response to rising TS*I*, and activate MLCK leading to recoil type retractions. At an average adhesion threshold, smaller increases in MLCK activity may be sufficient to induce pull type retractions, without SAC activation. Reduced MLCK activity can induce retraction by weakening adhesions below a minimum adhesion threshold, resulting in a release retraction. Continuous type retractions may occur at very low levels of TS*I* and independently of MLCK (open block arrow) when contractile forces are slightly higher than the minimum adhesion threshold. Thus the temporal regulation of detachment by MLCK can drive repeated cycles (curved arrows) of protrusion (P) and retraction (R). Meanwhile, increased Rho kinase activity (pale orange) at the cell rear provides spatial regulation of retraction by maintaining a constant, high, level of contractility in this region, throughout multiple cycles of motility.

retraction can occur independently of myosin II in cell types with very weak adhesions, a minimal level of contractility is clearly important for maintaining cytoskeletal cohesion that is required for normal movement [5].

Comparison of the effects of ML7, Y27632 and calcimycin treatment on the mechanics of detachment suggest that MLCK and Rho kinase provide temporal and spatial control of retraction. Our observation that increasing MLCK activity with calcimycin or decreasing it with ML7 can induce retraction provides evidence that calcium dependent regulation through MLCK is sufficient to regulate rear detachment. The speed with which modulation of MLCK can trigger retraction makes it a likely candidate for the temporal regulation of detachment. This is particularly important for fast moving cell types [33,36], because it can regulate adhesiveness on a time scale of seconds [50]. Furthermore, the activation of SACs within milliseconds and the subsequent calcium transients ensures a rapid response to a decrease in retraction rate. The role of Rho kinase in the spatial control of detachment is given by the rapid loss in cell polarity and negligible effect on retraction following Y27632 treatment. In addition, the increased protrusiveness at the rear of treated keratocytes is consistent with the well-documented role of Rho kinase in maintaining cortical tension, thereby inhibiting protrusion in this region. The slower kinetics of Rho kinase activity compared with MLCK [23] makes it particularly well suited for spatial regulation of detachment, since this would need to be maintained throughout multiple rounds of retraction. It is of interest that similar roles for MLCK and Rho kinase have been reported for fibrosarcoma cells [37].

The effects of inhibitor treatments illustrate the importance of maintaining contractile forces within narrow limits, so that detachment can occur at the rear without either excessive weakening or reinforcement of adhesions. Such “fine-tuning” of rear detachment rates is essential for maintaining a high degree of synchrony between protruding and retracting cell edges. Although the efficiency of retraction can be increased by lowering the adhesion threshold, large decreases in contractility following either ML7 or blebbistatin treatment leads to a temporary loss in cell polarity and a reduction in persistence of movement. Conversely, the large sustained increases in contractility following calyculin A treatment can induce detachment but they reduce retraction efficiency by raising the adhesion threshold. In addition, high contractile forces at the cell front inhibit protrusion, which results in a significant reduction in cell speed and persistence. Treatment with Y27632 also reduced cell speed and persistence. However, this was due to a loss in polarity, since the adhesion threshold, and retraction rate were unaffected. It is noteworthy that unlike other inhibitor treatments, calcimycin induced retraction without any net change in adhesion threshold, cell speed or persistence, which is consistent with its role regulating detachment.

We conclude that the separate roles of MLCK and Rho kinase in the control of retraction may be a general feature of rapidly moving cell types, because they need to retract frequently while maintaining polarity. This is only possible if the temporal and spatial regulation of retraction is under the control of different enzymes. The advantage of this type of regulation is that it allows cells to maintain rapid movement and to respond quickly to local

changes in adhesiveness. This is particularly important for rapidly moving cell types *in vivo* that traverse extracellular matrices of varying adhesiveness, stiffness, surface texture and dimensionality. Therefore, our observations in keratocytes may provide insight into the regulation of detachment *in vivo*, and during metastasis, since decreased adhesiveness together with increased motility occurs in both situations.

Acknowledgments

We thank C. Norris for assistance with confocal microscopy, and M. Dembo for a custom modification to the LIBTRC software. This work was supported by a National Science Foundation grant (Grant no. 0724147) to J.L.

REFERENCES

[1] M. Amano, M. Nakayama, K. Kaibuchi, Rho-kinase/ROCK: a key regulator of the cytoskeleton and cell polarity, Cytoskeleton 67 (2010) 545–554.
[2] K.I. Anderson, R. Cross, Contact dynamics during keratocyte motility, Curr. Biol. 10 (2000) 253–260.
[3] K.A. Beningo, K. Hamao, M. Dembo, Y.L. Wang, H. Hosoya, Traction forces of fibroblasts are regulated by the Rho-dependent kinase but not by the myosin light chain kinase, Arch. Biochem. Biophys. 15 (2006) 224–231.
[4] R.A. Brundage, K.E. Fogarty, R.A. Tuft, F.S. Fay, Calcium gradients underlying polarization and chemotaxis of eosinophils, Science 254 (1991) 703–706.
[5] Y. Cai, N.C. Gauthier, N. Biais, M.A. Fardin, X. Zhang, L.W. Miller, B. Ladoux, V.W. Cornish, M.P. Sheetz, Cytoskeletal coherence requires myosin IIA-dependent contractility, J. Cell Sci. 123 (2010) 413–423.
[6] W. Chen, Mechanism of retraction of the trailing edge during fibroblast movement, J. Cell Biol. 90 (1981) 187–200.
[7] W.T. Chen, Induction of spreading during fibroblast movement, J. Cell Biol. 81 (1979) 684–691.
[8] K. Clark, M. Langeslag, C.G. Figdor, F.N. van Leeuwen, Myosin II and mechanotransduction: a balancing act, Trends Cell Biol. (2007) 178–186.
[9] E. Crowley, A.F. Horwitz, Tyrosine phosphorylation and cytoskeletal tension regulate the release of fibroblast adhesions, J. Cell Biol. 131 (1995) 525–537.
[10] M. Dembo, Y.L. Wang, Stresses at the cell-to-substrate interface during locomotion of fibroblasts, Biophys. J. 76 (1999) 2307–2316.
[11] A. Doyle, W. Marganski, J. Lee, Calcium transients induce spatially coordinated increases in traction force during the movement of fish keratocytes, J. Cell. Sci. 117 (2004) 2203–2214.
[12] Doyle, A.D. 2004. Mechano-chemical signaling mechanisms in fish epidermal keratocytes. Dissertation. URL: ⟨http://search.proquest.com/docview/305209811⟩.
[13] A.D. Doyle, J. Lee, Cyclic changes in keratocyte speed and traction stress arise from Ca^{2+}-dependent regulation of cell adhesiveness, J. Cell Sci. 118 (2005) 369–379.
[14] G.A. Dunn, D. Zicha, Dynamics of fibroblast spreading, J. Cell Sci. 108 (1995) 1239–1249.
[15] R.J. Eddy, L.M. Pierini, F. Matsumura, F.R. Maxfield, Calcium-dependent myosin II activation is required for uropod retraction during neutrophil migration, J. Cell Sci. 113 (2000) 1287–1298.
[16] M.F. Fournier, S. Sauser, D. Ambrosi, J.-J. Meister, A. Verkhovsky, Force transmission in migrating cells, J. Cell Bio. 188 (2010) 287–297.
[17] M.L. Gardel, B. Sabass, L. Ji, G. Danuser, U.S. Schwarz, C.M. Waterman, Traction stress in focal adhesions correlates biphasically with actin retrograde flow speed, J. Cell Bio. 183 (2008) 999–1005.
[18] G. Giannone, P. Ronde, M. Gaire, J. Haich, K. Takeda, Calcium oscillations trigger focal adhesion disassembly in human U87 astrocytoma cells, J. Biol. Chem. 277 (2002) 26364–26371.
[19] W.H. Guo, Y.L. Wang, A three-component mechanism for fibroblast migration with a contractile cell body that couples a myosin II-independent propulsive anterior to a myosin II-dependent resistive tail, Mol. Biol. Cell 23 (2012) 1657–1663.
[20] Y. Iwadate, S. Yumura, Actin-based propulsive forces and myosin-II-based contractile forces in migrating Dictyostelium cells, J. Cell Sci. 121 (2008) 1314–1324.
[21] P.Y. Jay, P.A. Pham, K. Wong, E. Elson, A mechanical function of myosin II in cell motility, J. Cell Sci. 108 (1995) 387–393.
[22] C. Jurado, J.R. Haserick, J. Lee, Slipping or gripping? Fluorescent speckle microscopy in fish keratocytes reveals two different mechanisms for generating a retrograde flow of actin, Mol. Biol. Cell 16 (2005) 507–518.
[23] K. Katoh, Y. Kano, M. Amano, H. Onishi, K. Kaibuchi, K. Fujiwara, Rho-kinase-mediated contraction of isolated stress fibers, J. Cell Biol. 153 (2001) 569–583.
[24] K. Keren, Z. Pincus, G.M. Allen, E.L. Barnhart, G. Marriott, A. Mogilner, J.A. Theriot, Mechanism of shape determination in motile cells, Nature 453 (2008) 475–480.
[25] G. Kirfel, A. Rigort, B. Borm, V. Herzog, Cell migration: mechanisms of rear detachment and the formation of migration tracks, Eur. J. Cell Bio. 83 (2004) 717–724.
[26] J. Kolega, Asymmetric distribution of myosin IIB in migrating endothelial cells is regulated by a Rho-dependent kinase and contributes to tail retraction, Mol. Biol. Cell 14 (2003) 4745–4757.
[27] J. Lee, A. Ishihara, G. Oxford, B. Johnson, K. Jacobson, Regulation of cell movement is mediated by stretch-activated calcium channels, Nature 400 (1999) 382–386.
[28] J. Lee, K. Jacobson, The composition and dynamics of cell-substratum adhesions in locomoting fish keratocytes, J. Cell Sci. 110 (1997) 2833–2844.
[29] J. Lee, M. Leonard, T. Oliver, A. Ishihara, K. Jacobson, Traction forces generated by locomoting keratocytes, J. Cell. Biol. 127 (1994) 1957–1964.
[30] J. Limouze, A.F. Straight, T. Mitchison, J.R. Sellers, Specificity of blebbistatin an inhibitor of myosin II, J. Muscle Res. Cell Motil. 25 (2004) 337–341.
[31] M.L. Lombardi, D.A. Knecht, M. Dembo, J. Lee, Traction force microscopy in Dictyostelium reveals distinct roles for myosin II motor and actin-crosslinking activity in polarized cell movement, J. Cell Sci. 120 (2007) 1624–1634.
[32] M.L. Lombardi, D.A. Knecht, J. Lee, Mechano-chemical signaling maintains the rapid movement of Dictyostelium cells, Exp. Cell Res. 314 (2008) 1850–1859.
[33] P.W. Marks, F.R. Maxfield, Transient increases in cytosolic free calcium appear to be required for the migration of adherent human neutrophils, J. Cell Biol. 110 (1990) 43–52.
[34] R. Meili, B. Alonso-Latorre, d.A.J. C., R.A. Firtel, J.C. Lasheras, Myosin II is essential for the spatiotemporal organization of traction forces during cell motility, Mol. Biol. Cell 21 (2010) 405–417.
[35] S. Munevar, Y.L. Wang, M. Dembo, Distinct roles of frontal and rear cell-substrate adhesions in fibroblast migration, Mol. Biol. Cell 12 (2001) 3947–3954.
[36] T. Nebl, P.R. Fisher, Intracellular Ca^{2+} signals in Dictyostelium chemotaxis are mediated exclusively by Ca^{2+} influx, J. Cell. Sci. 110 (1997) 2845–2853.
[37] V. Niggli, M. Schmid, A. Nievergelt, Differential roles of Rho-kinase and myosin light chain kinase in regulating shape,

adhesion, and migration of HT1080 fibrosarcoma cells, Biochem. Biophys. Res. Commun. 343 (2006) 602–608.
[38] C.D. Nobes, A. Hall, Rho GTPases control polarity, protrusion, and adhesion during cell movement, J. Cell. Biol. 144 (1999) 1235–1244.
[39] S. Paku, J. Tovari, Z. Lorincz, F. Timar, B. Dome, L. Kopper, A. Raz, J. Timar, Adhesion dynamics and cytoskeletal structure of gliding human fibrosarcoma cells: a hypothetical model of cell migration, Exp. Cell Res. 290 (2003) 246–253.
[40] S.P. Palecek, A. Huttenlocher, A.F. Horwitz, D.A. Lauffenburger, Physical and biochemical regulation of integrin release during rear detachment of migrating cells, J. Cell Sci. 111 (Pt 7) (1998) 929–940.
[41] S.P. Palecek, C.E. Schmidt, D.A. Lauffenburger, A.F. Horwitz, Integrin dynamics on the tail region of migrating fibroblasts, J. Cell Sci. 109 (1996) 941–952.
[42] T. Pollard, G.G. Borisy, Cellular motility driven by assembly and disassembly of actin filaments, Cell 112 (2003) 453–465.
[43] B. Sabass, M.L. Gardel, C.M. Waterman, U.S. Schwarz, High resolution traction force microscopy based on experimental and computational advances, Biophys. J. 94 (2008) 207–220.
[44] Y. Sawada, M.P. Sheetz, Force transduction by triton cytoskeletons, J. Cell Bio. 156 (2002) 609–615.
[45] I.C. Schneider, C. Hays, C.M. Waterman, Epidermal growth factor-induced contraction regulates paxillin phosphorylation to temporally separate traction generation from de-adhesion, Mol. Biol. Cell 20 (2009) 3155–3167.
[46] L.B. Smilenov, A. Mikhailov, R.J. Pelham, E.E. Marcantonio, G.G. Gundersen, Focal adhesion motility revealed in stationary fibroblasts, Science 286 (1999) 1172–1174.
[47] L.A. Smith, H. Aranda-Espinoza, J.B. Haun, M. Dembo, D.A. Hammer, Neutrophil traction stresses are concentrated in the uropod during migration, Biophys. J. 92 (2007) L58–60.
[48] K.S.K. Uchida, T. Kitanishi-Yuimura, S. Yumura, Myosin II contributes to the posterior contraction and the anterior extension during the retraction phase in migrating Dictyostelium cells, J. Cell Sci. 116 (2003) 51–60.
[49] M. Vicente-Manzanares, X. Ma, R.S. Adelstein, A.R. Horwitz, Non-muscle myosin II takes centre stage in cell adhesion and migration, Nat. Rev. Mol. Cell. Biol. 10 (2009) 778–790.
[50] J.W. Walker, S.H. Gilbert, R.M. Drummond, M. Yamada, R. Sreekumar, R.E. Carraway, M. Ikeebe, F. Fay, Signaling pathways underlying eosinophil cell motility revealed by using caged peptides, Proc. Natl. Acad. Sci. USA 95 (1998) 1568–1573.
[51] D.J. Webb, K. Donais, L. Whitmore, S.M. Thomas, C.E. Turner, J.T. Parsons, A.F. Horwitz, FAK-Src signalling through paxillin, ERK and MLCK regulates adhesion disassembly, Nat. Cell Biol. 6 (2004) 154–161.
[52] C.A. Wilson, M.A. Tsuchida, G.M. Allen, E.L. Barnhart, K.T. Applegate, P.T. Yam, L. Ji, K. Keren, G. Danuser, J.A. Theriot, Myosin II contributes to cell-scale actin network treadmilling through network disassembly, Nature 465 (2010) 373–377.
[53] H. Wolfenson, A. Bershadsky, Y. Henis, B. Geiger, Actomyosin-generated tension controls the molecular kinetics of focal adhesions, J. Cell Sci. 124 (2011) 1425–1432.
[54] W.A. Worthylake, S. Lemoine, J.M. Watson, K. Burridge, RhoA is required for monocyte tail retraction during transendothelial migration, J. Cell Biol. 154 (2001) 147–160.